Exploring isospin, strangeness and charm distillation in nuclear collisions*

M. Reiter[a b], E. L. Bratkovskaya[a], M. Bleicher[a], W. Bauer[b], W. Cassing[c], H. Weber[a], and H. Stöcker[a]

[a]Institut für Theoretische Physik, Universität Frankfurt, 60054 Frankfurt, Germany

[b]Department of Physics, Michigan State University, East Lansing, MI, USA

[c]Institut für Theoretische Physik, Universität Giessen, 35392 Giessen, Germany

The isospin and strangeness dimensions of the Equation of State are explored. RIA and the SIS200 accelerator at GSI will allow to explore these regions in compressed baryonic matter. ^{132}Sn+^{132}Sn and ^{100}Sn+^{100}Sn collisions as well as the excitation functions of K/π, Λ/π and the centrality dependence of charmonium suppression from the UrQMD and HSD transport models are presented and compared to data. Unambiguous proof for the creation of a 'novel phase of matter' from strangeness and charm yields is not in sight.

The properties of neutron-rich matter at high densities and temperatures are largely unknown. Collisions of heavy rare isotopes provide an excellent tool to explore this unknown region in the phase diagram of nuclear matter. The planned Rare Isotope Accelerator (RIA) (up to $E_{\rm Lab} = 500$ AMeV) and the SIS200 at GSI (up to $E_{\rm Lab} = 30$ AGeV) are the upcoming experimental facilities that will access new energy density regions for these collisions allowing to investigate the Equation of State (EOS) of compressed hadronic matter in regions (2-10 $\rho_{\rm neutron}$) or even in directions ($n_{\rm neutron} = n_\Lambda$) which have not been experimentally accessible before.

Among the most interesting open questions is the isospin and strangeness dependency of the EOS, especially at high baryochemical potentials. This has been the subject of intensive research, as it is not only important in the study of radioactive nuclei but bears consequences on various important astrophysical issues as well [1]. The EOS of isospin asymmetric matter can be written as $e(\rho,\delta) = e(\rho,0) + E_{sym}(\rho)\delta^2 + O(\delta^4)$, where $\delta \equiv (\rho_n - \rho_p)/(\rho_n + \rho_p)$ is the isospin asymmetry, $e(\rho,0)$ is the energy density in isospin symmetric nuclear matter, and $E_{sym}(\rho)$ is a parametrisation for the isospin dependence of the nuclear symmetry energy [2]. Parametrisations for $E_{sym}(\rho)$ fall into two main categories [3]: (I) $E_{sym}(\rho)$ rises with ρ, (II) $E_{sym}(\rho)$ falls with increasing density ρ. The latter case has the interesting feature that symmetric matter may become unstable at high densities.

The (π^-/π^+) ratio is particularly sensitive to the high density behaviour of E_{sym} [4]. This can be easily understood qualitatively within the Δ resonance model for pion pro-

*Supported by DFG, BMBF, GSI and BCPL

duction [4]: Here first-chance independent nucleon-nucleon collisions [5] yield a primordial (π^-/π^+) ratio given by $(5N^2+NZ)/(5Z^2+NZ) \approx (N/Z)^2$. Thus, the charged pion ratio yields information on the isospin asymmetry (N/Z) in the dense participant matter, which depends on the high density behaviour of E_{sym} [4]. The (π^-/π^+) ratio can therefore be used to probe the EOS of neutron-rich nuclear matter.

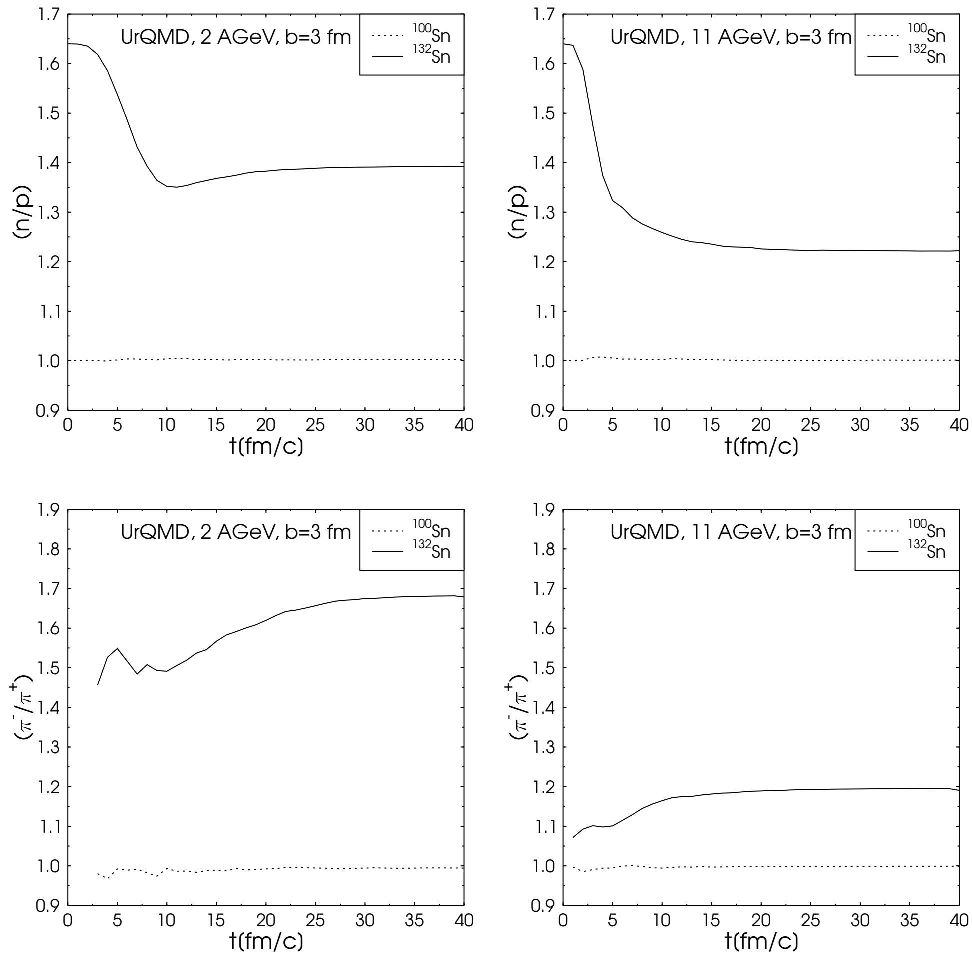

Figure 1. Time evolution of the (n/p) (top) and (π^-/π^+) (bottom) ratios in central ($b = 3$ fm) ^{132}Sn+^{132}Sn and ^{100}Sn+^{100}Sn collisions at 2 AGeV (left panels) and 11 AGeV (right panels) as calculated within the UrQMD model.

For our investigation of this effect the UrQMD model v1.2 [6,7] is applied to ^{132}Sn+^{132}Sn and ^{100}Sn+^{100}Sn collisions at 2 AGeV and 11 AGeV beam energy. Fig. 1 shows the time evolution of the (n/p) and (π^-/π^+) ratios. For ^{100}Sn+^{100}Sn, both the (n/p) and the (π^-/π^+) ratios are roughly time independent and of order one, as expected for the symmetric system. For the asymmetric system ^{132}Sn+^{132}Sn, the (n/p) ratio drops during the compression phase from its initial value of 1.64 and then saturates. At 2 AGeV, this saturation occurs after 15 fm/c at a value of (n/p) $\approx$ 1.4, whereas at 11 AGeV the saturation occurs earlier (10 fm/c) and to a lower final value of (n/p) $\approx$ 1.2.

The (π^-/π^+) ratio rises slightly during the early phase of the reaction and saturates rather later than (n/p) ($\sim 25-30$ fm/c at 2 AGeV and $\sim 15-20$ fm/c at 11 AGeV). The saturation values of ~ 1.7 (2 AGeV) and ~ 1.2 (11 AGeV) fall far below the first-chance Δ resonance model prediction $(N/Z)^2 \approx 2.7$. This is evident, as it is not the initial but rather the local and dynamically changing (n/p) ratio that determines the (π^-/π^+) ratio. In addition, pion reabsorptions and rescatterings reduce the sensitivity of (π^-/π^+) to (n/p). At higher energies, the increasing number of sequential nucleon-nucleon collisions drives the (π^-/π^+) ratio towards 1 via this mechanism.

For isospin-asymmetric matter, a distillation effect has recently been proposed [8], which is powered by chemical instabilities in the liquid-gas phase transition driving the system towards isospin symmetry. This effect is similar to the well-known *strangeness* distillation mechanism in nuclear reactions, which has been proposed as a quark-gluon-plasma (QGP) signal [9]. The search for the QGP and its properties has been a driving force behind years of relativistic heavy ion physics.

The fact that the Λ/π ratio and the K^+/π^+ ratio are found experimentally to exhibit a maximum at $E_{\rm Lab}$=10-30 AGeV and drop to half that value at 160 AGeV has raised speculations about the appearance of the 'new phase transition'. The NA49 Collaboration has recently started an energy scan at the SPS. First results are available now at 40 and 80 AGeV [10,11,12] and support these findings. Further studies are underway at 30 and 20 AGeV [13].

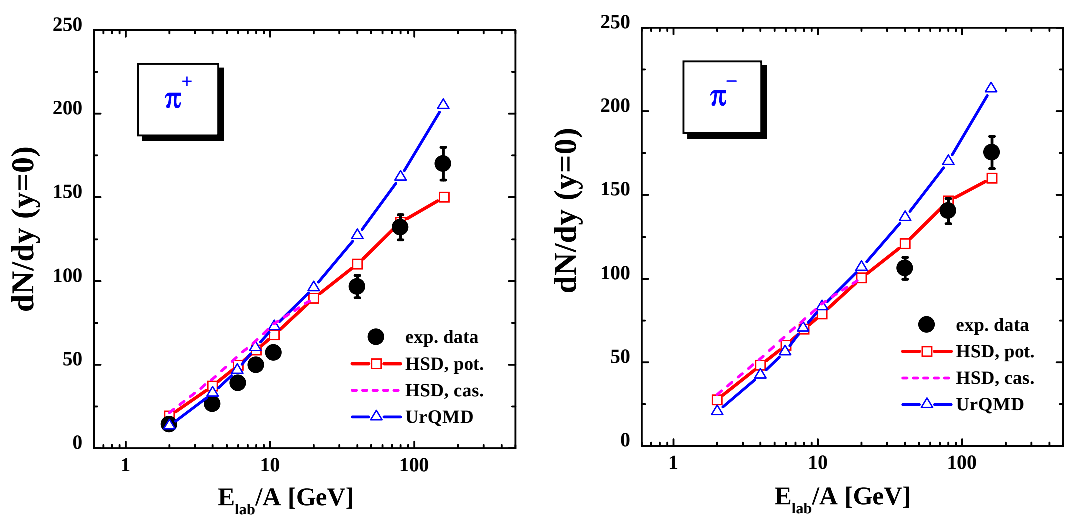

Figure 2. Excitation function of π^+ and π^- yields from central Au+Au (AGS) or Pb+Pb (SPS) collisions in comparison to experimental data [10,26]. Solid lines with open triangles show UrQMD results, solid lines with open squares and dashed lines stem from the HSD approach with and without potentials, respectively [23].

Let us discuss these maxima in the excitation function on the basis of 'conventional' hadron transport theories – do they exhibit analogous maxima? In that case, the interpretation of the data as a QGP signal becomes doubtful. The various hadron spectra are conventionally calculated with non-equilibrium kinetic transport theory (cf. [14,15,16,17, 18,19]). However, the calculated kaon to pion ratio from central nucleus-nucleus collisions turns out to vary by factors as large as 2 if different transport approaches are applied [19,20,21,22]. Thus a unique interpretation of the data is questionable so far.

Here we study the yields and ratios of protons, kaons, antikaons and hyperons from Au+Au (or Pb+Pb) collisions in the energy range from 1 AGeV to 160 AGeV [23]. The aim of this study is twofold: first, to find out the systematic differences between two currently used transport approaches (UrQMD [6,7] and HSD [14,24]), and second, to compare to related experimental data [10,11,12]. We provide predictions for experimental studies in the near future [13], which are also of relevance for the new GSI-proposal [25].

The two different transport models employed, i.e. the UrQMD v1.3 (here an updated version has been applied) and HSD approach have been used to describe nucleus-nucleus collisions from SIS to SPS energies for several years. Though different in the numerical realisation, both models are based on the same concepts: strings, quarks, diquarks ($q, \bar{q}, qq, \bar{q}\bar{q}$) accompanied by hadronic degrees of freedom. It is important to stress that both approaches do not include any explicit phase transition to a quark-gluon plasma (QGP). A common failure of both models in comparison to experimental data may – model independently – indicate the appearance of a novel state of strongly interacting matter.

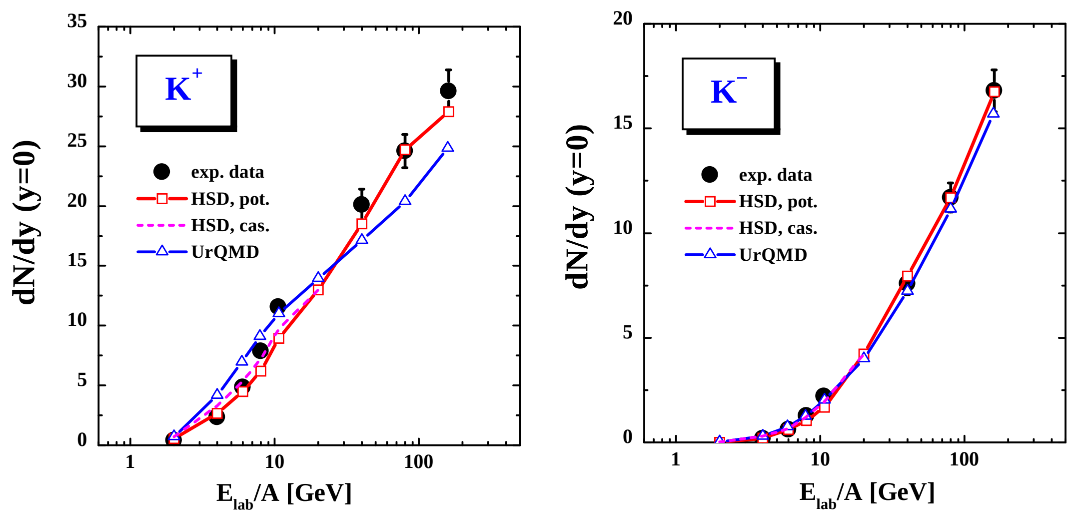

Figure 3. Excitation function of K^+ and K^- yields from central Au+Au (AGS) or Pb+Pb (SPS) collisions in comparison to experimental data [10,26]. Solid lines with open triangles show UrQMD results, solid lines with open squares and dashed lines stem from the HSD approach with and without potentials, respectively [23].

As a general overview on the $\pi^\pm$ abundancies in central Au+Au and Pb+Pb collisions Fig. 2 shows the π^+ and π^- multiplicities at mid-rapidity as a function of the bombarding energy in comparison to the available data [10,26]. Solid lines with open triangles show the results from the UrQMD calculations while the solid lines with open squares and dashed lines stem from the HSD approach with and without potentials, respectively. At lower AGS energies the UrQMD model gives slightly less pions then HSD (with/without potential), but both models overpredict the mid-rapidity data. Around 10 AGeV is the "crossing point" of both transport calculations and at SPS energies the tendency turns around: UrQMD gives more pions than HSD, so that HSD is now in a better agreement with the experimental data.

The K^+ and K^- multiplicities at mid-rapidity are depicted in Fig. 3 as a function of the beam energy in comparison to data from Refs. [10,26]: The K^- abundancies are well described by both transport models. The K^+ yield is slightly overestimated by UrQMD at AGS energies and underestimated at SPS energies, whereas HSD is in reasonable agreement with the data. Thus, Fig. 3 demonstrates that an underestimation of strangeness production is not the prevailing issue in comparison to the recent data from NA49 [10]. Both transport models can roughly describe - within their systematic range of uncertainties - the $K^\pm$ spectra and abundancies.

Fig. 4 contrasts the K^+/π^+ and K^-/π^- ratios at mid-rapidity as a function of energy for central collisions of Au+Au (AGS) or Pb+Pb (SPS) with the data [10,26]. The excitation function of the K^-/π^- ratio is roughly reproduced by both transport models, the maximum in the K^+/π^+ ratio seen experimentally is not described quantitatively by either HSD or UrQMD. For the K^+/π^+ ratio both models give quite different results. HSD gives a monotonous increase of this ratio with bombarding energy (in qualitative disagreement with the data as pointed out in Refs. [20,21]), whereas within UrQMD the ratio shows a maximum around 10 AGeV and then saturates to a slightly lower value towards RHIC energies, thus reproducing the behaviour of the data qualitatively. In view of Figs. 2 and 3 this failure is not primarily due to a mismatch of strangeness production, but more due to an insufficient description of the pion abundancies.

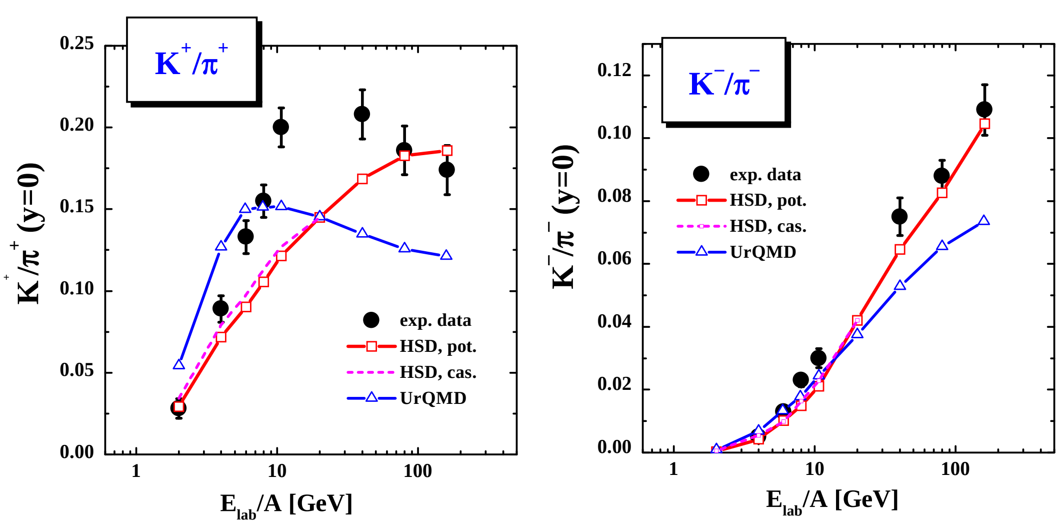

Figure 4. Excitation function of the K^+/π^+ and K^-/π^- ratios from central Au+Au (AGS) or Pb+Pb (SPS) collisions in comparison to experimental data [10,26]. Solid lines with open triangles show UrQMD results, solid lines with open squares and dashed lines stem from the HSD approach with and without potentials, respectively [23].

This overestimation of pion abundancies can be attributed to a number of reasons: One problem of the transport approaches used here is that detailed balance is not implemented for $n \leftrightarrow m$ transitions with $n, m \geq 3$ [27]. Thus multi-particle collisions might change the dynamical picture accordingly and lead to 'shorter' chemical equilibration times [28]. In fact, the importance of $3 \leftrightarrow 2$ transitions has been explored in an extended HSD transport approach [28] for antiproton reproduction by meson fusion for $A + A$ collisions at the AGS and SPS. In order to achieve a more conclusive answer from transport studies multi-particle interactions deserve further investigation in future generations of transport codes.

Another reason for the overestimation of the pion yield might be that the pions in both transport models are treated as 'free' particles, i.e. with their vacuum mass. Lattice QCD calculations and effective Lagrangian approaches like the Nambu-Jona-Lasinio (NJL) model however, indicate an increase in the pion mass with temperature and density. So the overestimation of the pion yields in HSD and UrQMD might be a signature for a dynamically larger pion mass. Moreover, in-medium changes of the strange hadron properties, as known from experimental studies at SIS energies, may also show up in the compressed baryonic matter encountered in the AGS and SPS energy range. Thus, including all medium effects simultaneously in a consistent way might provide a more conclusive interpretation of the ratios in Figs. 4 and 5. However, such calculations require a precise knowledge about the momentum and density dependence of the hadron self-energies which is not available so far.

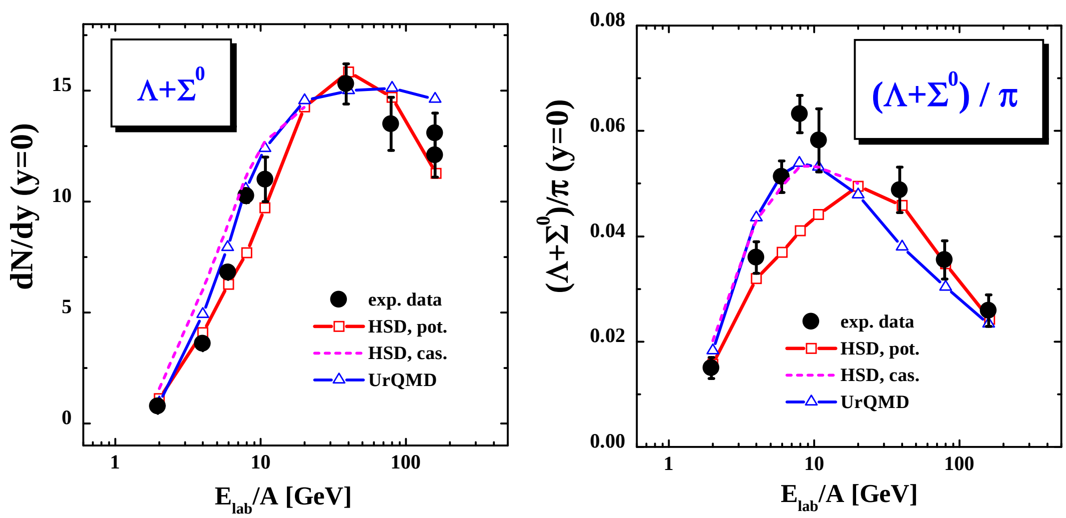

Figure 5. Excitation function of the $\Lambda + \Sigma^0$ yields and $(\Lambda + \Sigma^0)/\pi$ ratio from central Au+Au (AGS) or Pb+Pb (SPS) collisions in comparison to experimental data [10,26]. Solid lines with open triangles show UrQMD results, solid lines with open squares and dashed lines stem from the HSD approach with and without potentials, respectively [23].

Fig. 5 shows the excitation functions of $\Lambda + \Sigma^0$-hyperons (left) at mid-rapidity as a function of the bombarding energy for central collisions of Au+Au (AGS) or Pb+Pb (SPS) in comparison to data [11,12,29,30,31]. Here both models compare rather well with data. The $(\Lambda + \Sigma^0)/\pi$ ratios (right) at mid-rapidity are underestimated slightly which should again be attributed to the pion excess in the transport models (as discussed above). Nevertheless, the experimentally observed maxima in the ratios are qualitatively reproduced by both models, indicating that with increasing bombarding energy s-quarks are more frequently produced within mesons $(\overline{K}, \overline{K}^*)$ rather than in associate production with baryons. A similar trend is also found in statistical models [32].

What can we conclude from the common failures of the models studied in comparison

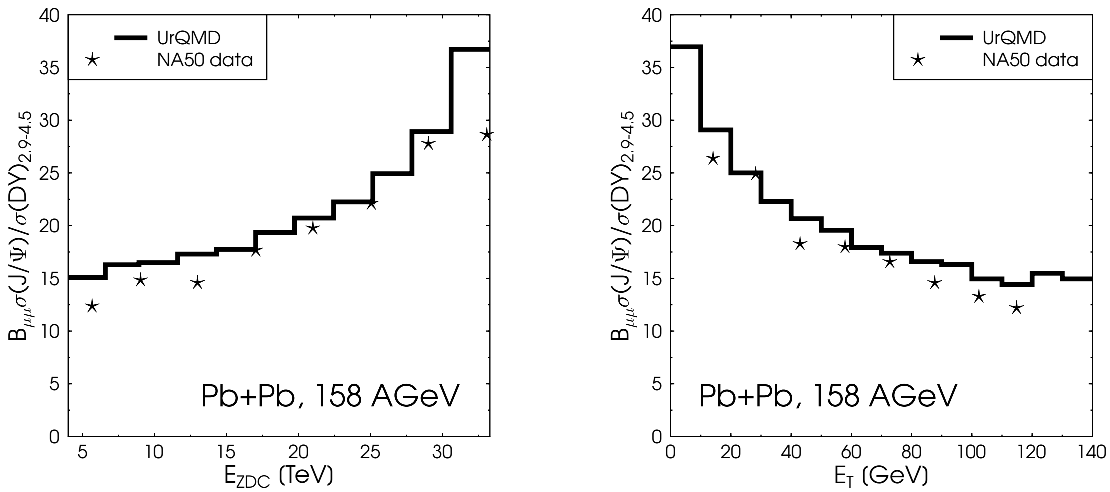

Figure 6. The ratio of J/Ψ to Drell-Yan production as a function of forward energy $E_{\rm ZDC}$ (left) and transverse energy $E_{\rm T}$ (right) in Pb+Pb collisions at 158 AGeV. Data points are preliminary results from the year 2000 NA50 Pb+Pb run [33], the histograms show the 1999 UrQMD results [34].

to related experimental data and does this failure provide evidence for a new state of matter in view of a QGP? In view of the large 'systematic uncertainties' in the discussed transport approaches we can quote an insufficient accuracy in the description of the pion degrees of freedom by both transport models. Thus, the deviations between theory and the data should not be seen as unambiguous signals for any kind of new physics.

Another much-discussed possible QGP signal is charmonium production. Here, new data on the $E_{\rm T}$ end $E_{\rm ZDC}$ dependence of J/Ψ production in Pb+Pb collisions at 158 AGeV from the year 2000 NA50 run has recently become available [33]. This data (one analysis), along with UrQMD results [34] (which are in line with HSD results [35]) is shown in Fig. 6. Note that the puzzling drop of the J/Ψ to Drell-Yan production at high E_T which was present in the 'old', previously available NA50 data is no longer present in the current NA50 data. The new NA50 data fall very close to the published UrQMD calculations by Spieles et al. [34]. To our opinion, both the $E_{\rm T}$ dependence and the $E_{\rm ZDC}$ dependence do no longer justify to speak of an 'anomalous' J/Ψ suppression in high energy heavy ion collisions.

We have shown that the exploration of the isospin and strangeness dimensions of the Equation of State opens fascinating new areas of research. Especially the upcoming experimental possibilities like the planned Rare Isotope Accelerator RIA and the SIS200 machine at GSI will allow to explore novel phenomena in compressed baryonic matter in great detail. While conclusive unambiguous proof for the creation of a 'novel phase of matter', e. g. Quark Gluon Plasma, from strangeness and charm yields is still lacking, the hunt and quest for it has provided new insights and even opened novel fields of research. It has become a driving force behind modern high energy nuclear physics.

Acknowledgement

We thank A. Kostyuk, L. Gerland, R. Vogt, and L. Csernai for many fruitful discussions.

REFERENCES

1. J. Schaffner-Bielich, M. Hanauske, H. Stöcker and W. Greiner, astro-ph/0005490.
2. R. B. Wiringa, V. Fiks and A. Fabrocini, Phys. Rev. C **38** (1988) 1010.
3. J. Margueron, J. Navarro, N. Van Giai and W. Jiang, nucl-th/0110026.
4. B. A. Li, Phys. Rev. Lett. **88** (2002) 192701; B. A. Li, nucl-th/0301039. B. A. Li, Phys. Rev. C **67** (2003) 017601 B. A. Li, Nucl. Phys. A **708** (2002) 365
5. R. Stock, Phys. Rept. **135** (1986) 259.
6. S.A. Bass et al., Prog. Part. Nucl. Phys. **42**, 279 (1998).
7. M. Bleicher et al., J. Phys. G **25**, 1859 (1999).
8. M. Di Toro et al., nucl-th/0301033.
9. C. Greiner and H. Stöcker, Phys. Rev. D **44** (1991) 3517.
10. S.V. Afanasiev et al. (NA49 Collab.), Phys. Rev. C. **66** (2002) 054902
11. A. Mischke et al. (NA49 Collab.), J. Phys. G. **28**, 1761 (2002).
12. A. Mischke et al. (NA49 Collab.), nucl-ex/0209002, to be published in Nucl. Phys. A.
13. The NA49 Collaboration, Addendum-10 to Proposal CERN/SPSC/P264.
14. W. Cassing and E. L. Bratkovskaya, Phys. Rep. **308**, 65 (1999).
15. H. Stöcker and W. Greiner, Phys. Rep. **137**, 277 (1986).
16. G. F. Bertsch and S. Das Gupta, Phys. Rep. **160**, 189 (1988).
17. W. Cassing, V. Metag, U. Mosel, and K. Niita, Phys. Rep. **188**, 363 (1990).
18. C. M. Ko and G. Q. Li, J. Phys. G **22**, 1673 (1996).
19. F. Wang, H. Liu, H. Sorge, N. Xu, and J. Yang, Phys. Rev. C **61**, 064904 (2000).
20. W. Cassing, E. L. Bratkovskaya, S. Juchem, Nucl. Phys. A **674**, 249 (2000).
21. J. Geiss, W. Cassing, and C. Greiner, Nucl. Phys. A **644**, 107 (1998).
22. H. Weber, E.L. Bratkovskaya, and H. Stöcker, Phys. Lett. B **545**, 285 (2002).
23. H. Weber, E. L. Bratkovskaya, W. Cassing and H. Stöcker, Phys. Rev. C **67** (2003).
24. W. Ehehalt and W. Cassing, Nucl. Phys. A **602**, 449 (1996).
25. http://www.gsi.de/GSI-Future/cdr/.
26. L. Ahle et al. (E866 and E917 Collab.), Phys. Lett. B **476**, 1 (2000); Phys. Lett. B **490**, 53 (2000).
27. M. Belkacem et al., Phys. Rev. C **58**, 1727 (1998); L.V. Bravina et al., Phys. Lett. B **434**, 379 (1998); L.V. Bravina et al., J. Phys. G **25**,351 (1999); L.V. Bravina et al., Phys. Rev. C **60**, 024904 (1999).
28. W. Cassing, Nucl. Phys. A **700**, 618 (2002). R. Rapp and E. V. Shuryak, Phys. Rev. Lett. **86**, 2980 (2001). C. Greiner and S. Leupold, J. Phys. G **27**, L95 (2001).
29. S. Ahmad et al. (E891 Collab.), Phys. Lett. B **382**, 35 (1996); C. Pinkenburg et al. (E866 Collab.), Nucl. Phys. A **698**, 495c (2002).
30. S. Albergo et al., (E896 Collab.), Phys. Rev. Lett. **88**, 062301 (2002).
31. F. Antinori at al. (WA97 Collab.), Nucl. Phys. A **661**, 130c (1999).
32. P. Braun-Munzinger, J. Cleymans, H. Oeschler and K. Redlich, Nucl. Phys. A **697**, 902 (2002).
33. L. Ramello, (NA50 Collab.), talk given at QM2002
34. C. Spieles, R. Vogt, L. Gerland, S. A. Bass, M. Bleicher, H. Stöcker and W. Greiner, Phys. Rev. C **60** (1999) 054901
35. W. Cassing and E. L. Bratkovskaya, Nucl. Phys. A **623** (1997) 570